ADVANCES IN MATERIALS SCIENCE, Vol. 22, No. 2 (72), June 2022

DOI: 10.2478/adms-2022-0004

Muhammed Fatih Kilicaslan[1,] *, Saad Ibrahim Elburni[2], Yasin Yilmaz[3], Mehmet Akkaş[4]

[1]Department of Fundamental Sciences and Engineering, Sivas University of Science and Technology, 58000, Sivas, Turkey
[2]Department of Materials Science and Engineering, Kastamonu University, 37000, Kastamonu, Turkey
[3]Department of Aeronautical Engineering, Sivas University of Science and Technology, 58000, Sivas, Turkey
[4]Department of Mechanical Engineering, Kastamonu University, 37000, Kastamonu, Turkey

***** *fatihkilicaslan@sivas.edu.tr*

EFFECTS OF B ADDITION ON THE MICROSTRUCTURE AND MICROHARDNESS OF MELT-SPUN Al-7075 ALLOY

ABSTRACT

Main aim of this study is to examine change of microstructural and the mechanical properties of Al-7075 alloy depending on B content added with different proportions. Rapid solidification process used to produce the alloys was carried out with a single roll melt spinner via a wheel with a rotational speed of 25 m/s. For the microstructural characterization of the alloys, a scanning electron microscope and X-ray diffraction analyzes were used. According to obtained results, it can be said that B addition led to modification of dimensions and shapes of both α−Al and intermetallic phases occurred, it reduced average grain size from 0.45 μm to 0.34 μm in the microstructure. The B addition also led to dramatically increase in microhardness of the Al-7075 alloy. The microhardness of the alloy with 0.4 wt. % B is 0.19 GPa, this is clearly one times higher than that of the alloy without B addition. The microhardness of the alloy with 1 wt. % B is 0.21 GPa, this is also slightly higher than that of the alloy with 0.4 wt. % B.

Keywords: *Al-7075; B addition; microhardness; microstructure; rapid solidification*

INTRODUCTION

Aluminum and its alloys are one of the most abundant engineering materials on the earth and have a traditional and versatile range of applications. They owe this advantage to their properties such as superior corrosion resistance, excellent machinability, high strength-to-density ratio i.e. specific strength, and favorable thermal and electrical conductivity [1]. Thanks to these properties possessed by them, aluminum alloys have become suitable for the production of structural and industrial components such as automotive parts and military equipment [2]. Apart from these interesting properties; superior performance, design perspective, reasonable production costs and

well-known manufacturing techniques reveal why the Al alloys are preferred more often than other metal alloys in the manufacturing sector [3]. Considering the above-mentioned properties of the aluminum alloys, 7000 series (Al-Zn-Mg-Cu) aluminum alloys are mostly known as the aluminum alloys with the excellent mechanical strength [4–8]. In addition to this advantage, the 7000 series aluminum alloys stand out with their properties such as good ductility [9,10], corrosion resistance [9–12] and weldability [7,10,13]. These properties enable them to play a significant role in divergent industries such as aviation, automotive etc. [7,8,11,14–17]. The high strength of the 7000 series aluminum alloys can be clarified mainly by the strength contribution of nano-sized secondary phase particles together Guinier-Preston zones, η^I and η phases, which are formed during aging process immediately after solution hardening process in precipitation hardening process [4,18–21]. In addition to the precipitation hardening, other different mechanisms such as cold deformation [22–24], grain boundary hardening [6,25], semi-solid casting [7,26,27] can also contribute to the mechanical strength. Along with improving the mechanical strength with the aforementioned mechanisms, various researchers are working on adding various impurity elements and/or using new production methods such as rapid solidification techniques in order to modify the microstructure of the Al alloys [9,15,35–37,16,28–34]. Various impurity elements as an inoculant agent are used to provide grain refinement and obtain a microstructure having homogeneous distribution and minimum segregation in the Al alloys [38]. In order to refine the grain size in the aluminum alloys, melt inoculation is performed by using mostly aluminum master alloys containing Ti and/or B [39]. In a study by Alipour et al., the effect of Al-8B grain refiner on the microstructure of an Al-based, Al-12Zn-3Mg-2.5Cu alloy was investigated. Here, it was observed that Al-8B grain refiner was as effective as possible in refining the microstructure grains. Here, it is emphasized that AlB_2 phase particles in the Al-8B grain refiner master alloy, which is a strong heterogeneous nucleation site for the Al, are effective in refining columnar, coarse α-Al grains in the microstructure of the alloy into equiaxed α-Al grains [40]. In a study made by Wang et al., the effect of an Al-Ti-B type grain refiner master alloy on the grain size in commercial purity Al was investigated. The obtained results showed that TiB_2 particles in the Al-Ti-B master alloy refined the α-Al particles by forming solid solutions of Al_3Ti and (Ti, Al)B_2 intermetallics [41]. Srinivasan et al., investigated how Zr addition affects the microstructure of the alloy in the Al-Si-Zr alloy system, in their study. Accordingly, they observed that the intermetallic phases of Al_3Zr (with tetragonal DO_2 structure) and orthorhombic Si_2Zr, which occur in the microstructure with the Zr addition, effectively providing heterogeneous nucleation sites, promote grain refining [35]. Leng et al. investigated the effect of Sc and the Zr added to the 7075 Al alloy (Al-Zn-Cu-Mg) on the microstructure. They concluded that Al_3(Sc, Zr) intermetallic particles, which promote grain refinement in the microstructure with the Sc and the Zr addition, play a role in heterogeneous nucleation [34]. In recent years, the rapid solidification techniques are also of great interest owing to their ability to modify the microstructure of the alloys significantly and furthermore to achieve superior mechanical properties with their ability to form amorphous microstructures [37]. Thanks to the rapid solidification processes, the grain refinement can be effectively triggered by obtaining high-density nuclei in the microstructure of the alloys [4,42,43]. Melt spinning method, which is one of the rapid solidification methods, comes into prominence due to its relatively high cooling rates (10^5-10^7 K/s) and mass production advantage [38,42–44]. Spraying a homogeneous molten metal alloy onto a rotating copper wheel and rapidly solidifying into a thin ribbon are steps during the process. High solidification rates increase solute concentrations, by suppressing

their atomic motion [33]. When existing studies in the literature are examined, it is striking that the melt spinning method is used in the production of various aluminum-based alloys [4,37,45–49]. The melt spinning process offers a number of beneficial aspects for the Al alloys, such as increased dispersoid fraction due to higher solute atom content [15,50], finer grain size [50], shorter distance between adjacent precipitate particles and dislocations during plastic deformation [51], slightly improved precipitate nucleation caused by deformation-induced faults [52]. The microstructural and chemical composition differences between rapid solidifying zone and slow solidifying zone in traditional production methods constitute a disadvantage in the alloys. Therefore, in the rapid solidification methods such as the melt spinning process, the entire alloy microstructure solidifies simultaneously and very quickly, which provides a microstructure with homogeneous composition [38]. Additionally, B introduced into the alloy, creates more nucleation sites in the microstructure through the heterogeneous nucleation mechanism together with the rapid solidification process [40] and provides a more homogeneous and finer grained microstructure with the formation of some seconder intermetallic phases [41]. Besides these, the rapid solidification process makes the diffusion of the B introduced into the alloy difficult, leading to the formation of a supersaturated solid solution in terms of the B and a severe plastic deformation. When the aforementioned studies on the improvement of the microstructural and the mechanical properties of the Al-alloys are examined in the literature, the studies about the effects of the B addition on the microstructural and the mechanical properties of the Al-7075 alloy obtained by the rapid solidification processes are not available or quite limited. Hence, our main purpose is to examine the contribution of the B addition to the microstructural and mechanical properties of the Al-7075 alloy, which is produced by the melt spinning method. In this way, combined effect of the melt spinning method and the B addition on the microstructural and the mechanical properties of 7075 Al alloy, which is widely used in aviation (for example production of structural material in commercial and military aircrafts [53]), is revealed. Compared to conventional manufacturing methods, a microstructure with much finer grain was obtained with the melt spinning method with the B addition was observed compared to the 7075 Al alloy without the B addition.

EXPERIMENTAL

A mixture of high purity alloying elements (99.99 wt. %Al, 99.99 wt. % Zn, 99.99 wt. %Mg, 99.99 wt. %Fe, 99.99 wt. % Cu, 99.99 and 99.99 wt. %Cr) was used in the production of the alloys containing three different wt. % B contents, as base-AlZnMgFeCu, AlZnMgFeCu0.4B and AlZnMgFeCu1B alloys respectively. Ferro-boron (FeB) master alloy with a grain size distribution range of 0.4-3.5 mm was used as B additive. Nominal chemical compositions of the alloys are shown in Table 1. In order to produce the above-mentioned alloys, firstly, alloy ingots were obtained by conventional casting method by means of an induction furnace. They are then cut into small pieces for use in the melt spinning process. Finally, the alloy ingots were melted in the melt spinning process at 750 ^{o}C and sprayed under pressure onto a rotational brass wheel (250 mm diameter and approximately 20 m/s rotational speed) at 700 ^{o}C via a 2 mm wide nozzle. The molten alloys sprayed onto cylindrical surface of the wheel was drawn from the surface of the wheel as ribbons approximately 1-10 mm wide and 10-30 μm thick. Some details of the melt spinning process of the Al-7075 alloys with different B content are shown in Fig.1. For the

microstructural examination of the alloys produced in the ribbon forms, some specimens taken from each alloys were embedded in epoxy resin separately for polishing and etching processes. Keller's solution (2 ml HF + 3 ml HCl + 5 ml HNO_3 + 190 ml H_2O), which has a very important place for aluminum alloys, was used in the etching process in the microstructural examination of the specimens. Then, microstructural and surface examination of the specimens were characterized by FEI Quanta FEG 250 scanning electron microscopy (SEM), SEM-Energy dispersive spectrometry (EDS) and a Bruker D8 Advance X-ray diffractometry (XRD) devices, while their microhardness tests were performed by static micro-indentation analysis using Vicker's microhardness device (while the applied load during the microhardness test is 100 gf, the holding time is 15 s). In this study, melt-spun base-AlZnMgFeCu, AlZnMgFeCu0.4B and AlZnMgFeCu1B alloys are coded as AAM00, AAM-0.4B and AAM-1B, respectively. Table 1 shows the chemical composition of each melt-spun Al-alloy achieved in the study in wt. %. All the experimental studies and tests mentioned above were carried out in the rapid solidification laboratory of Kastamonu University. The grain size measurements in the microstructures were tried to be determined through SEM micrographs of each alloy with the help of a program called SEM Afford.

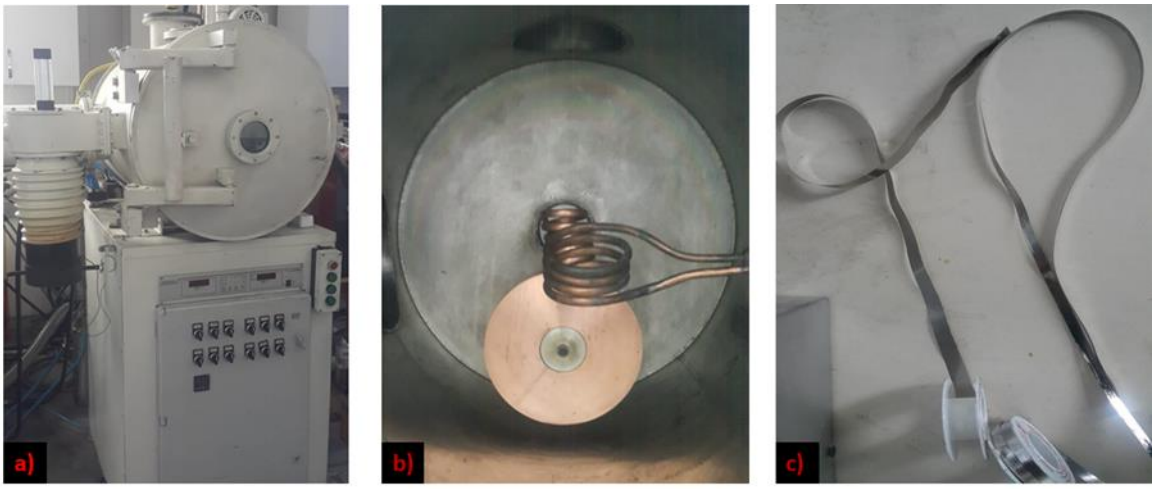


Fig. 1. Some details of the melt spinning process of the Al-7075 alloys: a) Outher section of the melt spinning machine. b) Injecting the molten aluminum alloy into the copper rotary wheel. c) Ribbon-shaped, base Al-7075 alloy produced about in ~ 8 mm width and ~ 20 μm thickness

Table 1. *The chemical composition of produced melt-spun Al-7075 alloys with different B content of AAM00, AAM-04B and AAM-1B respectively (wt. %)*

Alloy specimen	Al	Zn	Si	Cu	Mn	Mg	Cr	Ti	B	Fe
AAM00	bal.	6.52	0.727	1.64	0.053	2.48	0.263	0.095	-	0.115
AAM-1B	bal.	6.52	0.727	1.64	0.053	2.48	0.263	0.095	0.1	0.115
AAM-04B	bal.	6.52	0.727	1.64	0.053	2.48	0.263	0.095	0.4	0.115

RESULTS AND DISCUSSION

Fig. 2 shows the optical microscope (OM) images of the base Al-7075 alloy (without the B addition) and the Al-7075 alloys containing 0.4 wt.% and 1 wt.% B in as cast. According to Fig. 2a), the OM image of the base Al-7075 alloy (coded as AAM00) shows relatively coarse microstructure. As shown in Fig. 2b), the OM image of the Al-7075 alloy with 0.4 wt.% B (coded as AAM-04B) shows finer microstructure than that of the AAM00 alloy. According to Fig. 2c), which shows the OM image of Al-7075 alloy with 1 wt.% B (coded as AAM-1B), as the B content increases much more, homogeneously distributed, finer sized, smoother grains appeared in the microstructure. As a result, it can be said that the B addition to the Al-7075 alloy causes a gradual decrease in the size of the α-Al phases. In addition, thanks to the B, the distribution of the α-Al phases in the microstructure became more homogeneous and their shapes changed from an irregular form to a equiaxed one. There are some factors that make the distribution of the phases in the microstructure to be more homogeneous and finer can be listed as follows: Firstly, as known, supercooling rate of the alloy during the solidification is inversely proportional to the size of the grains formed in the microstructure, that is, as the nucleation rate increases, the size of the newly formed grains decreases [39]. Accordingly, it can be said that the rapid cooling used in the melt spinning method refines the size of the grains formed in the microstructure. In fact, it is possible to achieve almost nano-sized grains with this method [25,45]. Another factor can be that during the rapid solidification, the B introduced into the alloy increases the nucleation region in the microstructure with heterogeneous nucleation mechanism, thus forms the finer and the equiaxed grains [40]. In this way, the supercooling required for the nucleation is reduced. In a study by Alamdari et al., when a B-based innoculant was used to refine the grain size in the microstructure of an Al-alloys, a finer and more homogeneous microstructure having α-Al was achieved via TiB_2 particles [54]. In another study by Wang et. al., a homogeneous microstructure having finer grain size was achieved via some secondary intermetallic phases such as $(Al,Ti)B_2$ using the Al-Ti-B master alloy as an innoculant i.e. grain refiner for the heterogeneous nucleation mechanism [41]. Additionally, it can be mentioned that the rapid cooling process makes long-distance diffusion of the B introduced into the alloy difficult, causing the formation of supersaturated solid solution and severe lattice distorsion in the α-Al lattice, leading to a decrease in grain size. This situation is presented in a study by Shang et al. [55].

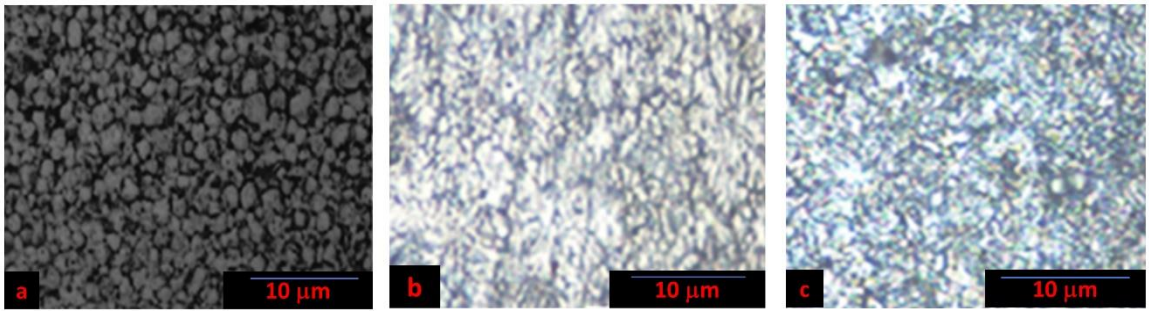


Fig. 2. The OM images of the melt-spun Al-7075 alloys: a) AAM00, b) AAM-04B and c) AAM-1B alloy respectively

Fig. 3a) shows the XRD patterns for the melt-spun alloys with different B content AAM00, AAM-04, and AAM-1B respectively. Accordingly, only well-defined α-Al-crystal peaks are seen in all of the alloys, and there is no clear peaks of any intermetallic phase. We predict that the absence of any intermetallic phase in our current study is probably due to very fine dimensions of them caused by effect of the rapid cooling during the melt spinning process and/or very low proportions in the microstructures as stated also by Prakah et. al and Kılıçaslan et al. [38,56]. On the other hand, as seen in Fig. 3b), the enlarged XRD patterns of the melt-spun Al alloys, with the B addition, the α-Al peaks seem to shift to the right, in other words, they occur at larger 2θ angles. This situation can be explained by some factors: The atomic radii of the B element added to the α-Al crystal lattice (0.853 Å) is lower than that of the Al matrix atom to which it is added (1.230 Å) [57]. Therefore, according to the Bragg's Law, the distance between crystalline atomic planes, "d", and consequently the lattice parameter, "a", decreases with the addition of an element with a relatively smaller atomic diameter than that of the matrix atom. This is the case in a study by Xu et al. [58]. In addition, as stated in a study by Otriz et al., depending on the atomic radii and type of the alloying element introduced into the α-Al lattice (here, element B is added.), it can be associated with the formation of Al-based solid solution with lower lattice parameters [59]. In a study by Wang et al., this case has happened [41]. In addition, the increase in α-Al peak width with the B element introduced into the α-Al lattice can mean the decrease in the grain size in the microstructure [55,59]. Additionally, it is thought that 0.11 wt.% Fe content in the composition of the alloy can dissolve in the Al-lattice and form a solid solution. When the SEM-EDS analysis in Fig. 5 is investigated, EDS spot numbers of 1, 2 and 3 contains 0.45, 0.16 and 0.17 wt.% Fe respectively and these are considerably less compared to the Al content. Therefore, from this SEM-EDS analysis, it can be said that the Fe content is introduced to the Al-lattice and forms a solid solution. This can be supported with the studies by Kılıçaslan et al. [38] and Wang et al. [60].

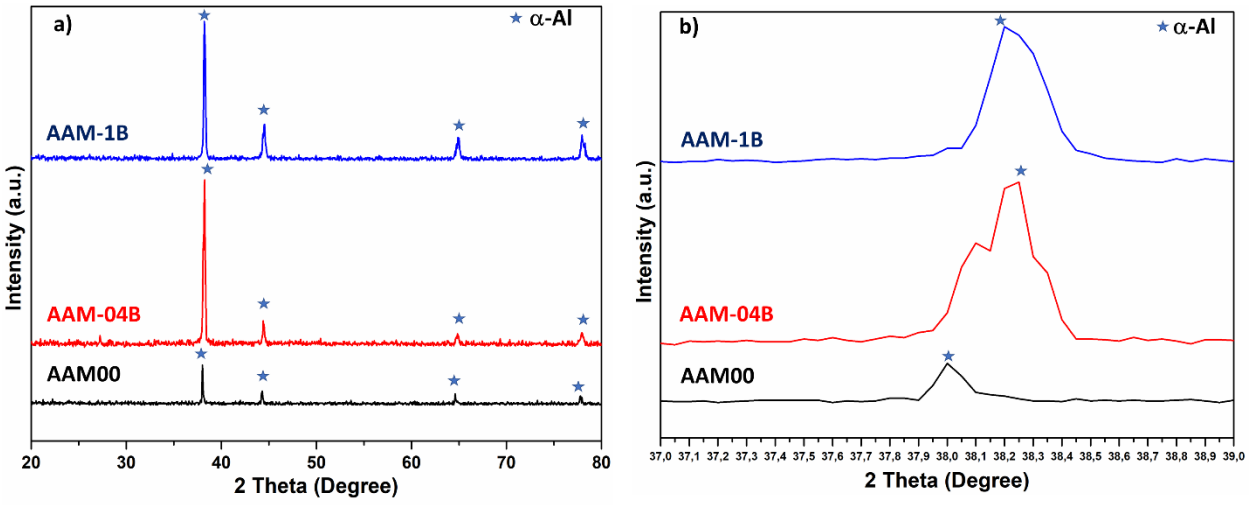


Fig. 3. a) The XRD patterns taken from the melt-spun AAM00, AAM-04B, and AAM-1B alloys respectively. b) The XRD patters taken form the melt-spun AAM00, AAM-04B and AAM-1B alloys indicating the shift of the α-Al peaks

The SEM images of the melt spun alloys are shown in Fig. 4. Fig. 4.a) presents the microstructure and relatively large grain structure at the grain boundaries of the base AAM00 alloy, where the size of α-Al grains varies between 0.14 μm and 2.44 μm, and average grain size is 0.45 μm. Additionally, some particle-like secondary phase grains having relatively coarse grain size are seen in the microstructure. Fig. 4.b) presents the microstructure of the AAM-04B alloy. Here, we notice that with the addition of 0.4 wt.% B, the shape of the secondary phases buried in the Al lattice transforms to include both particle-like and rectangular, blocky shaped phases.

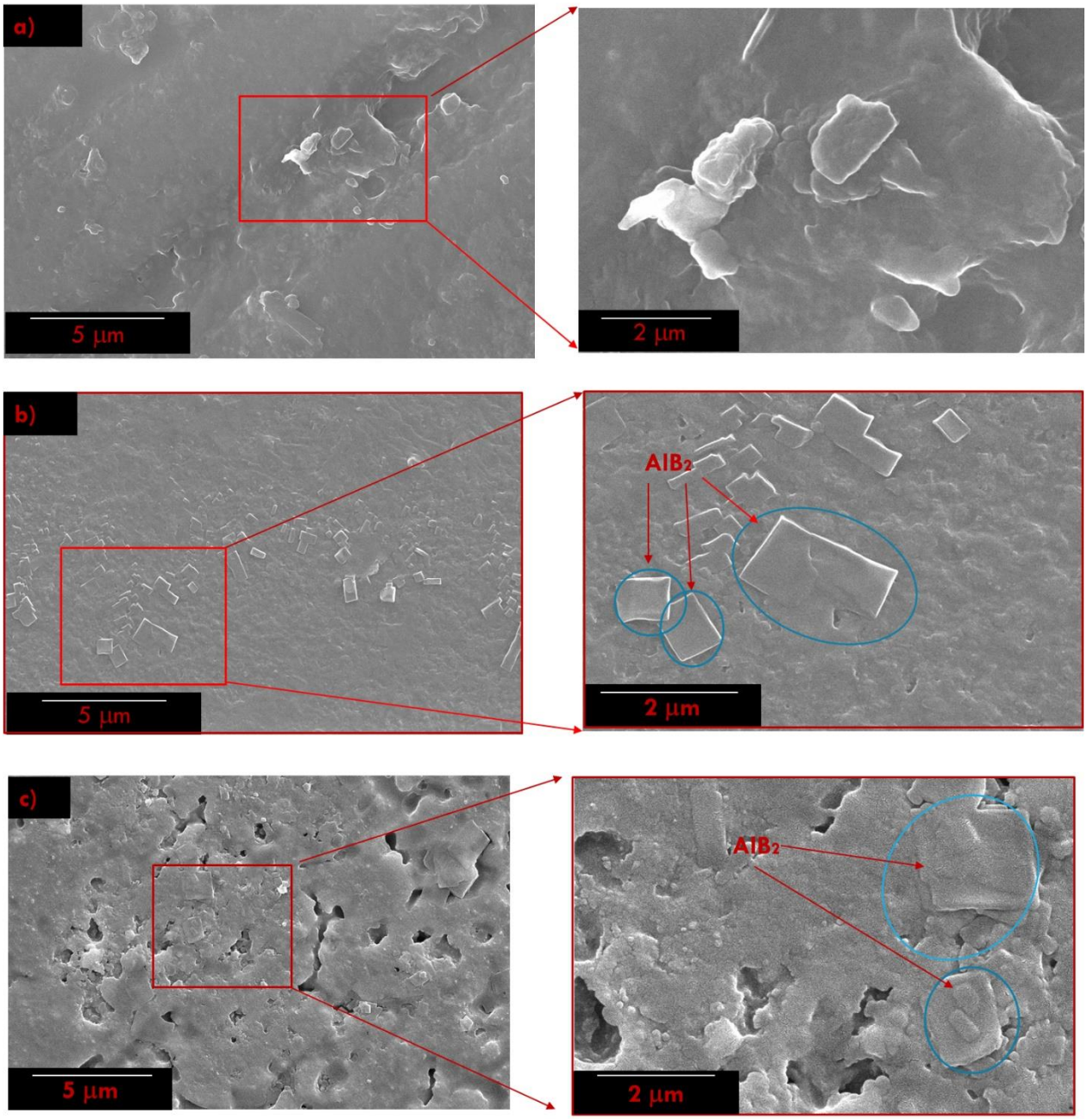


Fig. 4. The SEM images revealing the microstructure of melt-spun AAM00 (a), AAM-04B (b), and AAM-1B (c) alloys respectively

Besides, it is seen that homogeneity in the distribution of the alloying elements, which made the α-Al grains finer (here the grain size is between 0.44 μm and 2.03 μm and average grain size is around 0.42 μm.) than that of the base alloy, hence, the average grain size of the α-Al decreases. Fig. 4.c) presents the microstructure of the AAM-1B alloy which clearly indicates equiaxed, spherical α-Al grains (here the grain size is between 0.14 μm and 1.66 μm and average grain size is around 0.34 μm.) finer, together with some rectangular shaped secondary phases coarser than that of AAM-04B alloy. Hence, it can be said that as the B content added to the alloy increases, average grain size of the α-Al lattice in the microstructure decreases. Here, the microstructure of the alloy, which clearly indicates smooth grains and homogeneity in distribution of them with clarity of the grain boundaries, this can be supported by the Hall-Petch theory, which states that as the grain size decreases, the grain boundary increases per unit volume [42]. Additionally, it was revealed as a fine polygonal structure which is mainly composed of α-Al phase (light phase) and intermetallic phase (dark phase). As concluded by Wang [60], the borides appear as dark particles in a bright Al-lattice because the atomic number of the B is less than that of aluminum atoms and thus generates fewer scattered electrons than the Al-lattice. The vast majority of boride particles have a rectangular shape. The boride particles collect within the aluminum matrix to form clusters. Additionally, as we mentioned above before, we predicted that solid solubility limit of the B in the alloy may have increased as a result of the rapid solidification process. The sizes and shapes of the clusters indicate that the majority of the boride particles are dispersed within the α-Al grains.

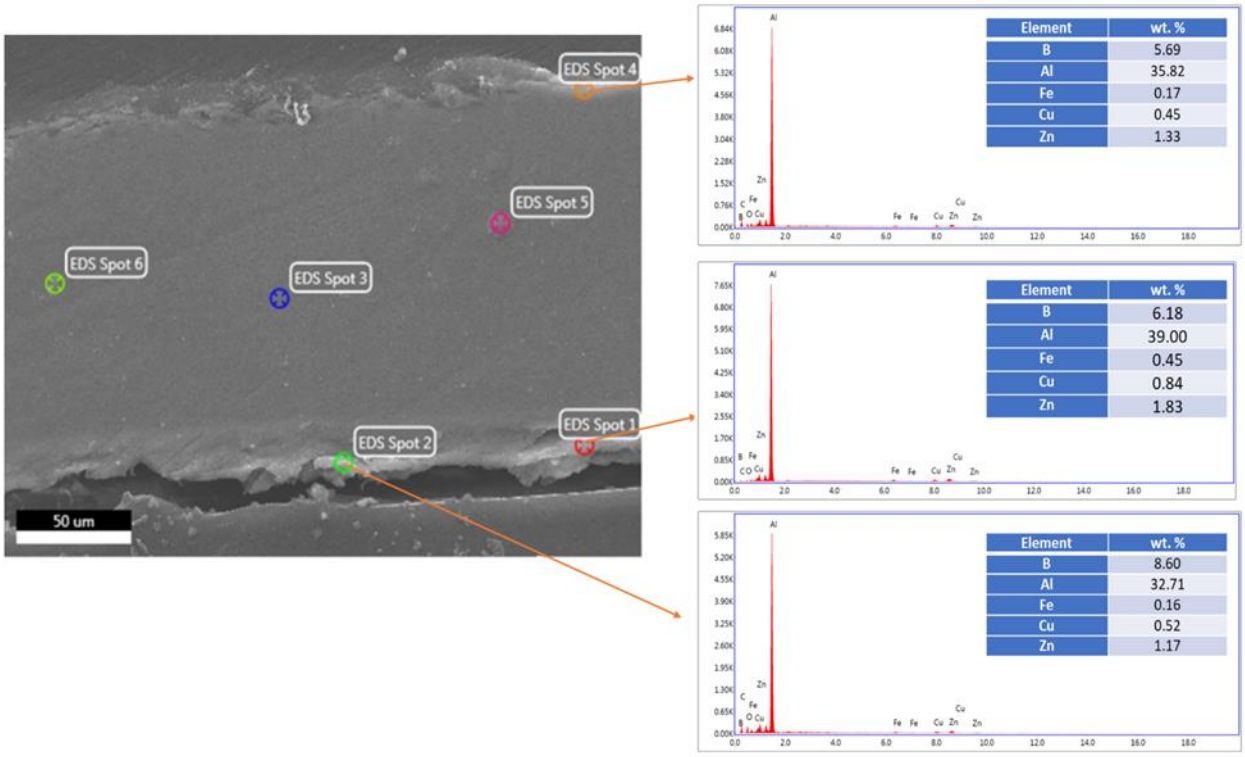


Fig. 5. The SEM-EDS analysis from the melt-spun AAM-04B alloy

When the SEM-EDS results in Fig. 5 are investigated, it is seen that B element is introduced into the microstructure of the alloy. As a result of EDS spot number 2, which is predicted to be a nano-sized intermetallic phase, the B ratio has increased to 8.60 wt. %, for the AAM-04B alloy. This result shows that there may be AlB_2 intermetallic phase in the microstructure of the alloys according to the result obtained by Chen et. al in the grain refinement of Al-Si casting alloys by adding La and the B into the microstructure of the alloys [58]. The same result was obtained in another study where Al-Ti-B master alloys was used as a grain refiner by Wang et. al. [41].

Table 2. shows the average microhardness values of melt-spun Al-7075 alloys containing different B content. As seen here, the B addition into the alloy significantly increased the microhardness of it. Accordingly, the addition of 0.4 wt. % B (in the AAM-04B alloy) increased the microhardness to 0.19 GPa that is clearly greater than that of the base alloy of 0.1 GPa. On the other hand, the addition of 1 wt. %B (in the AAM-1B alloy) increased the microhardness to 0.21 GPa that is slightly higher than that of the AAM-04B alloy. The factors that increase the microhardness, as mentioned above before can be listed that the B addition forms a solid solution in the microstructure and its solid solubility limit increases as a result of rapid cooling and accordingly, the distortion occurs in the crystal lattice and grain size decreases. Moreover, the fact that the B addition, which is introduced into the microstructure as an inoculant, plays a role in the heterogeneous nucleation process also causes the grain size to be refined, hence, an increase in the microhardness occurs, according to the Hall-Petch's theory [42], as stated above before.

Table 2. *The microhardness values of the melt spun AAM00, AAM-04B and AAM-1B alloys depending on different B content*

Alloy	Microhardness (HV_{100}), GPa
AAM00	0.1
AAM-04B	0.19
AAM-1B	0.21

CONCLUSIONS

The effects of the B addition on the microstructural and mechanical characteristics of the melt spun Al-7075 alloy is reported in this work. The B addition revealed these findings as follows:

- It continually refined the grain size of the α-Al phases, additionally the α-Al phase distributions were more uniform, and their forms changed from an irregular to an equiaxed forms.
- It increased the size of the secondary phases in the matrix and changed their sharp-edged particle-like structure from to a rectangular shaped structure.

- It also led to a significant increase in the microhardness. The alloy containing 1 wt. % B had the highest microhardness that was about one time higher than that of the base alloy. The mechanisms increasing the microhardness were attributed to the rapid cooling process, the solid solution formation, the severe lattice distortion and the grain refinement mechanisms as stated above before.
- The findings showed that there is an opportunity to produce the ribbon shaped alloy with very thin thickness of 15-20 μm. Moreover, the mechanical properties of the melt-spun alloy was improved beside the microstructural properties by the rapid solidification process.

ACKNOWLEDGEMENT

Authors would like to thank to University of Kastamonu / Department of Engineering and Material Science, for supporting this work.

Conflicts of Interest

The authors declare that they have no competing financial interests or personal relationships that could have seem to influence the study reported in this paper.

REFERENCES

1. A. Azarniya, A.K. Taheri, K.K. Taheri, Recent advances in ageing of 7xxx series aluminum alloys: A physical metallurgy perspective, J. Alloys Compd. 781 (2019) 945–983. https://doi.org/10.1016/j.jallcom.2018.11.286.
2. A. Azarniya, H.R.M. Hosseini, A new method for fabrication of in situ Al/Al_3Ti-Al_2O_3 nanocomposites based on thermal decomposition of nanostructured tialite, J. Alloys Compd. 643 (2015) 64–73. https://doi.org/10.1016/j.jallcom.2015.04.145.
3. E.A. Starke, J.T. Staleyt, Application of modern aluminum alloys to aircraft, Pro. Aerosp. Sci. 32 (1996) 131–172. https://doi.org/10.1016/0376-0421(95)00004-6.
4. Y. Lin, S. Mao, Z. Yan, Y. Zhang, L. Wang, Melt spinning induces sub-micrometric/ micrometric grained structure and dislocations in 7075 Al alloy, J. Alloys Compd. 651 (2015) 699–704. https://doi.org/10.1016/j.jallcom.2015.08.146.
5. M.B. Lezaack, F. Hannard, L. Zhao, A. Orekhov, J. Adrien, A. Miettinen, H. Idrissi, A. Simar, Towards ductilization of high strength 7XXX aluminium alloys via microstructural modifications obtained by friction stir processing and heat treatments, Materialia. 20 (2021) 101248. https://doi.org/10.1016/j.mtla.2021.101248.
6. D.Z. Avery, B.J. Phillips, C.J.T. Mason, M. Palermo, M.B. Williams, C. Cleek, O.L. Rodriguez, P.G. Allison, J.B. Jordon, Influence of Grain Refinement and Microstructure on Fatigue Behavior for Solid-State Additively Manufactured Al-Zn-Mg-Cu Alloy, Metall. Mater. Trans. A. 51 (2020) 2778–2795. https://doi.org/10.1007/s11661-020-05746-9.

7. J. Fu, K. Wang, X. Li, H. Zhang, Microstructure evolution and thixoforming behavior of 7075 aluminum alloy in the semi-solid state prepared by RAP method, Int. J. Miner. Metall. Mater. 23 (2016) 1404–1415. https://doi.org/10.1007/s12613-016-1364-3.
8. K.W. J. Fu, H. Jiang, Influence of Processing Parameters on Microstructural Evolution and Tensile Properties for 7075 Al Alloy Prepared by an ECAP-Based SIMA Process, Acta Metall. Sin. 31 (2018) 337–350. https://doi.org/10.1007/s40195-017-0672-6.
9. X. Meng, D. Zhang, W. Zhang, C. Qiu, D. Chen, Materials Science & Engineering A Achieving high damping capacity and strength simultaneously in a high-zinc aluminum alloy via melt spinning and hot extrusion, Mater. Sci. Eng. A. 833 (2022) 142376. https://doi.org/10.1016/j.msea.2021.142376.
10. P. Wang, H.C. Li, K.G. Prashanth, J. Eckert, S. Scudino, Selective laser melting of Al-Zn-Mg-Cu: Heat treatment, microstructure and mechanical properties, J. Alloys Compd. 707 (2017) 287–290. https://doi.org/10.1016/j.jallcom.2016.11.210.
11. E.T.A. Guner, D. Dispinar, Microstructural and Mechanical Evolution of Semisolid 7075 Al Alloy Produced by SIMA Process at Various Heat Treatment Parameters, Arab. J. Sci. Eng. 44 (2019) 1243–1253. https://doi.org/10.1007/s13369-018-3477-7.
12. W. Wang, J. Shen, W. Liu, H. Bian, Q. Li, Effect of laser energy density on surface physical characteristics and corrosion resistance of 7075 aluminum alloy in laser cleaning, Opt. Laser Technol. 148 (2022) 107742. https://doi.org/10.1016/j.optlastec.2021.107742.
13. X. Su, G. Xu, J. Jiang, Structural and mechanical properties of 7075 alloy strips fabricated by roll-casting in a static magnetic field, Int. J. Miner. Metall. Mater. 21 (2014) 696–701. https://doi.org/10.1007/s12613-014-0960-3.
14. J. Leng, B. Ren, Q. Zhou, J. Zhao, Effect of Sc and Zr on recrystallization behavior of 7075 aluminum alloy, Trans. Nonferrous Met. Soc. China. 31 (2021) 2545–2557. https://doi.org/10.1016/S1003-6326(21)65674-1.
15. X. Meng, D. Zhang, W. Zhang, C. Qiu, G. Liang, Microstructure and mechanical properties of a high-Zn aluminum alloy prepared by melt spinning and extrusion, J. Alloys Compd. 819 (2020) 152990. https://doi.org/10.1016/j.jallcom.2019.152990.
16. X. Meng, D. Zhang, W. Zhang, C. Qiu, G. Liang, Influence of solution treatment on microstructures and mechanical aluminum alloy, Mater. Sci. Eng. A. 802 (2021) 140623. https://doi.org/10.1016/j.msea.2020.140623.
17. X. Meng, D. Zhang, W. Zhang, C. Qiu, G. Liang, Microstructure and mechanical properties of a rapidly-solidified and extruded Al-13.2 Zn-2.5 Mg− 1.2 Cu-0.2 Zr alloy and its aging hardening response at 120°C, Mater. Sci. Eng. A. 826 (2021). https://doi.org/10.1016/j.msea.2021.141969.
18. R.D.P. Adler, Calorimetric Studies of 7000 Series Aluminum Alloys: II. Comparison of 7075, 7050, and RX720 Alloys, Metall. Trans. A. 8 (1977) 1185–1190. https://doi.org/10.1007/BF02667404.
19. J.K. Park, A.J. Ardell, Precipitate microstructure of peak-aged 7075 Al, Scr. Metall. 22 (1988) 1115-1119. https://doi.org/10.1016/S0036-9748(88)80114-5.
20. P.N. Adler, R. Deiasi, G. Geschwind, Influence of Microstructure on the Mechanical Properties and Stress Corrosion Susceptibility of 7075 Aluminum Alloy, Metall. Trans. 3 (1972) 3191-3200. https://doi.org/10.1007/BF02661333.

21. A.H. Feng, D.L. Chen, Z.Y. Ma, Microstructure and Cyclic Deformation Behavior of a Friction-Stir-Welded 7075 Al Alloy, Metall. Mater. Trans. A. 41 (2010) 957–971. https://doi.org/10.1007/s11661-009-0152-3.

22. Z.M. El-Baradie, M. El-Sayed, Effect of double thermomechanical treatments on the properties of 7075 A1 alloy. J. Mater. Process. Technol. 62 (1996) 76-80. https://doi.org/10.1016/0924-0136(95)02226-0.

23. Y.H. Zhao, X.Z. Liao, Z. Jin, R.Z. Valiev, Y.T. Zhu, Microstructures and mechanical properties of ultrafine grained 7075 Al alloy processed by ECAP and their evolutions during annealing. Acta Mater. 52 (2004) 4589–4599. https://doi.org/10.1016/j.actamat.2004.06.017.

24. Y.H. Zhao, X.Z. Liao, Y.T. Zhu, Enhanced mechanical properties in ultrafine grained 7075 Al alloy. J. Mater. Res. 20 (2005) 288-291. https://doi.org/10.1557/JMR.2005.0057.

25. L. Greer, Grain refinement in rapidly solidified alloys. Metals (Basel). 133 (1991) 16–21. https://doi.org/10.1016/0921-5093(91)90006-9.

26. U. A. Curle, G. Govender, Semi-solid rheocasting of grain refined aluminum alloy 7075. Trans. Nonferrous Met. Soc. China. 20 (2010) 832–836. https://doi.org/10.1016/S1003- 6326(10)60590-0.

27. Ł. Rogal, J. Dutkiewicz, H.V. Atkinson, L. Lity, T. Czeppe, M. Modigell, Characterization of semi-solid processing of aluminium alloy 7075 with Sc and Zr additions. Mater. Sci. Eng. A. 580 (2013) 362–373. https://doi.org/10.1016/j.msea.2013.04.078.

28. D. Srinivasan, K. Chattopadhyay, Metastable phase evolution and hardness of nanocrystalline Al–Si–Zr alloys. Mater. Sci. Eng. 306 (2001) 534–539. https://doi.org/10.1016/S0921-5093(00)01510-0.

29. S. Liu, X. Wang, Q. Zu, B. Han, X. Han, C. Cui, Significantly improved particle strengthening of Al–Sc alloy by high Sc composition design and rapid solidification. Mater. Sci. Eng. A. 800 (2021) 140304. https://doi.org/10.1016/j.msea.2020.140304.

30. Y. Lin, S. Mao, Z. Yan, Y. Zhang, L. Wang, The enhanced microhardness in a rapidly solidified Al alloy. Mater. Sci. Eng. A. 692 (2017) 182–191. https://doi.org/10.1016/j.msea.2017.03.052.

31. L.L. Rokhlin, T.V. Dobatkina, N.R. Bochvar, E.V. Lysova, Investigation of phase equilibria in alloys of the Al–Zn–Mg–Cu–Zr–Sc system. J. Alloys Compd. 367 (2004) 10–16. https://doi.org/10.1016/j.jallcom.2003.08.003.

32. G. Peng, K. Chen, H. Fang, S. Chen, A study of nanoscale Al3(Zr, Yb) dispersoids structure and thermal stability in Al–Zr–Yb alloy. Mater. Sci. Eng. A. 535 (2012) 311–315. https://doi.org/10.1016/j.msea.2011.12.094.

33. D.S. Thompson, B.S. Subramanya, S.A. Levy, Quench Rate Effects in AI-Zn-Mg-Cu Alloys. Metall. Trans. 2 (1971) 1149–1160. https://doi.org/10.1007/BF02664247.

34. K.E. Knipling, D.C. Dunand, D.N. Seidman, Precipitation evolution in Al – Zr and Al – Zr – Ti alloys during aging at 450–600 °C. Acta Mater. 56 (2008) 1182–1195. https://doi.org/10.1016/10.1016/j.actamat.2007.11.011.

35. Y. Yang, J.J. Licavoli, S.A. Hackney, P.G. Sanders, Coarsening behavior of precipitate Al3(Sc,Zr) in supersaturated Al-Sc-Zr alloy via melt spinning and extrusion. J. Mater. Sci. 56 (2021) 11114–11136. https://doi.org/10.1007/s10853-021-05981-4.

36. Y. Yang, J.J. Licavoli, P.G. Sanders, Improved strengthening in supersaturated Al-Sc-Zr alloy via melt- spinning and extrusion. J. Alloys Compd. 826 (2020) 154185. https://doi.org/10.1016/j.jallcom.2020.154185.

37. M. Vlach, V. Kodetova, J. Cizek, M. Leibner, F. Luk, L. Bajtošov, H. Kudrnov, V. Sima, S. Zikmund, E. Cernoskova, P. Kutalek, V. Neubert, V. Neubert, Role of Small Addition of Sc and Zr in Clustering and Precipitation Phenomena Induced in AA7075. Metals (Basel). 22 (2021) 1–20. https://doi.org/10.3390/met11010008.

38. M.F. Kilicaslan, S.I. Elburni, B. Akgul, The effects of Nb addition on the microstructure and mechanical properties of melt spun Al-7075 alloy. Adv. Mater. Sci. 21 (2021) 16–25. https://doi.org/10.2478/adms-2021-0008.

39. S. Murty, S.A. Kori, M. Chakraborty, B. S. Murty, S. A. Kori, M. Chakraborty, Grain refinement of aluminium and its alloys by heterogeneous nucleation and alloying. Int. Mater. Rev. 47 (2013) 1–29. https://doi.org/10.1179/095066001225001049.

40. M. Alipour, M. Azarbarmas, F. Heydari, M. Hoghoughi, M. Alidoost, M. Emamy, The effect of Al–8B grain refiner and heat treatment conditions on the microstructure, mechanical properties and dry sliding wear behavior. J. Mater. Des. 38 (2012) 64–73. https://doi.org/10.1016/j.matdes.2012.02.008.

41. X. Wang, Z. Liu, W.E.I. Dai, Q. Han, On the understanding of aluminum grain refinement by Al-Ti-B type master alloys. Metall. Mater. Trans. B. 2 (2014) 1620–1625. https://doi.org/10.1007/s11663-014-0252-3.

42. E.J. Lavernia, T.S. Srivatsan, The rapid solidification processing of materials: science, principles, technology, advances, and applications. J. Mater. Sci. 45 (2010) 287–325. https://doi.org/10.1007/s10853-009-3995-5.

43. H. Jones, A perspective on the development of rapid solidification and nonequilibrium processing and its future. Mater. Sci. Eng. 304–306 (2001) 11–19. https://doi.org/10.1016/s0921-5093(00)01552-5.

44. M.F. Kılıçaslan, Y. Yılmaz, B. Akgül, H. Karataş, C.D. Vurdu, Effect of Fe-Ni substitution in FeNiSiB soft magnetic alloys produced by melt spinning. Adv. Mater. Sci. 21 (2021) 79–89. https://doi.org/10.2478/adms-2021-0026.

45. K. Dehghani, M. Salehi, M. Salehi, H. Aboutalebi, Comparing the melt-spun nanostructured aluminum 6061 foils with conventional direct chill ingot. Met. Sci. Eng. 489 (2008) 245–252. https://doi.org/10.1016/j.msea.2007.12.017.

46. Z. Chen, J. Zhao, P. Chen, Microstructure and mechanical properties of nanostructured A8006 ribbons. Mater. Sci. Eng. A. 552 (2012) 189–193. https://doi.org/10.1016/j.msea.2012.05.029.

47. M. Salehi, K. Dehghani, Structure and properties of nanostructured aluminum A413.1 produced by melt spinning compared with ingot microstructure. J. Alloys Compd. 457 (2008) 357–361. https://doi.org/10.1016/j.jallcom.2007.03.117.

48. G.L. Litynska-Dobrzynska, J. Dutkiewicz, W. Maziarz, Microstructure of rapidly solidified Al-12Zn-3Mg-1.5Cu alloy with Zr and Sc additions. Mater. Trans. 52 (2011) 309–314. https://doi.org/10.2320/matertrans.MB201009.

49. K.S. Prasad, A.K. Mukhopadhyay, B. Majumdar, D. Akhtar, K.S. Prasad, A.K. Mukhopadhyay, B. Majumdar, D. Akhtar, On the nature and stability of phases present in a rapidly solidified aluminium alloy 7010 containing scandium. Mater. Manuf. Process. 6914 (2008) 658–664. https://doi.org/10.1080/10426910802316633.

50. M.S.W. Szymanski, M. Bigaj, M. Gawlik, M. Mitka, Consolidation by continuous rotary extrusion of aluminum cast by the melt spinning process. Arch. Metall. Mater. 59 (2014) 309–312. https://doi.org/10.2478/amm-2014-0050.

51. D. Srinivasan, K. Chattopadhyay, Formation and coarsening of a nanodispersed microstructure in melt spun Al–Ni–Zr alloy. Mater. Sci. Eng. A. 255 (1998) 107–116. https://doi.org/10.1016/S0921-5093(98)00769-2.

52. N. Berndt, P. Frint, Influence of extrusion temperature on the aging behavior and mechanical 24 properties of an AA6060. Metals (Basel). 8 (1) (2018) 1–9. https://doi.org/10.3390/met8010051.

53. T. Dursun, C. Soutis, Recent developments in advanced aircraft aluminium alloys, J. Mater. Des. 56 (2014) 862–871. https://doi.org/10.1016/j.matdes.2013.12.002.

54. H.D. Alamdari, D. Dubé, P. Tessier, Behavior of boron in molten aluminum and its grain refinement mechanism. Metall. Mater. Trans. A. 44 (2013) 388–394. https://doi.org/10.1007/s11661-012-1388-x.

55. H. Shang, B. Ma, K. Shi, R. Li, G. Li, The strengthening effect of boron interstitial supersaturated solid solution on aluminum films. Mater. Lett. 192 (2017) 104–106. https://doi.org/10.1016/j.matlet.2016.12.048.

56. P.B. Prakash, K.B. Raju, K. Venkatasubbaiah, N. Manikandan, Microstructure analysis and evaluation of mechanical propertiesof Al 7075 GNP's composites. Mater. Today Proc. 5 (2018) 14281–14291. https://doi.org/10.1016/j.matpr.2018.03.010.

57. S. Kohiki, M. Nishitani, T. Wada, Enhanced electrical conductivity of zinc oxide thin films by ion implantation of gallium, aluminum, and boron atoms. J. Appl. Phys. 75 (1994) 2069–2072. https://doi.org/10.1063/1.356310.

58. Z.Q. Xu, Z.L. Ma, M. Wang, Y.W. Chen, Y.D. Tan, X.W. Cheng, Design of novel lowdensity refractory high entropy alloys for high-temperature applications. Mater. Sci. Eng. A. 755 (2019) 318–322. https://doi.org/10.1016/j.msea.2019.03.054.

59. A.L. Ortiz, L. Shaw, X-ray diffraction analysis of a severely plastically deformed aluminum alloy. Acta Mater. 52 (2004) 2185–2197. https://doi.org/10.1016/j.actamat.2004.01.012.

60. F. Wang, D. Qiu, Z.L. Liu, J.A. Taylor, M.A. Easton, M.X. Zhang, Crystallographic study of grain refinement of Al by Nb addition, J. Appl. Crystallogr. (2014). https://doi.org/10.1107/S1600576714004476.